*Int. J. Electrochem. Sci.*, 11 **(2016)** 4779 – 4793, doi: 10.20964/2016.06.7

**International Journal of ELECTROCHEMICAL SCIENCE**
www.electrochemsci.org

# Preparation and Evaluation of a Stable Solid State Ion Selective Electrode of Polypyrrole/Electrochemically Reduced Graphene/Glassy Carbon Substrate for Soil Nitrate Sensing

*Pu Pan*[1,3], *Zhang Miao*[1,*], *Li Yanhua*[1], *Zhang Linan*[2], *Ren Haiyan*[1], *Kong Pan*[2], *Pan Linpei*[2]

[1] Key Laboratory on Modern Precision Agriculture System Integration Research of Ministry of Education, China Agricultural University, Beijing 100083, China
[2] Key Lab of Agricultural Information Acquisition Technology, China Agricultural University, Beijing 100083, China
[3] Northwest Agriculture and Forestry University, Yang ling 712100, China
[*]E-mail: zhangmiao@cau.edu.cn

*Received:* 15 February 2016 / *Accepted:* 2 April 2016 / *Published:* 4 May 2016

In this study, a stable solid state sensor was developed for soil nitrate detection, which was based on the molecular imprinting principle using polypyrrole doped with nitrate (PPy-$NO_3^-$) as the ion-selective membrane. Firstly, a theoretical analysis was conducted to confirm that a water layer formation between ion selective membrane and substrate was the key reason to response potential drift then a graphene layer was introduced as a hydrophobic solid contact layer by electrochemical reduction of graphene oxide onto the surface of glass carbon electrode (GCE). Finally, a PPy-$NO_3^-$ film was modified on the GR layer by a pulsed electro-polymerization technique and the novel nitrate sensor was finished. The physical and electrochemical properties of obtained sensor were detailed by different characterization methods then a real soil detection was carried out to evaluate the sensor performance in practical application. It was found that the graphene layer could restrain the water layer formation and promote ion-to-electron transition effectively, which would enhance the output stability and response rate significantly. For the sensor, many expected performances were presented such as higher stability, sensitivity and selectivity, etc., which was indicated by a negligible potential drift (0.67±0.05 $mV \cdot h^{-1}$), higher Nernstian slope (56.2±0.2 $mV \cdot decade^{-1}$), wide linear range ($10^{-5}$–$10^{-1}$ M), satisfied detection limit ($10^{-5.2\pm0.1}$ M) and a shorter response time (≤15 s). In real soil detection, the satisfactory results support its availability in agriculture application.

**Keywords:** Nitrate sensor; molecular imprinting technique; polypyrrole; graphene

## 1. INTRODUCTION

Nitrate nitrogen the most important kind of nitrogen fertilizer is crucial for agricultural industry. As affecting crop yield, the concept that the more fertilizer input the larger profit receiving is

very popular especially in the developing country[1]. Overuse fertilizer is becoming a serious issue in agriculture field. A report from the National Statistics Bureau reveals that in China the total chemical fertilizer consumption has increased more than 3.5 times in the past 30 years rocketing to 59.12 million tons in 2013. However there is only 1.5-fold growth for total grain production. Besides the common negative impacts caused by overuse fertilizer (e.g., soil degradation, resource waste, cost soar for production), some new ones have drawn much attention especially in environment protection and food safety. Since the negative charged nitrate cannot be held by soil particles, they will be enriched in surface and ground water at last by runoff leaching, which is the main inducement of eutrophication-algae blooms[2]. Anthony Butler has point that gastric cancer could be induced easily by excessive nitrate in food and drinking water as the formation of carcinogenic nitrosamines in acidic conditions of stomach[3]. The relationship between nitrate in drinking water and bladder cancer was also stated by Nadia Espejo-Herrera et al.[4] Therefore, it is urgent to the determine nitrate in soil to adjust fertilizer application reasonably.

Although many advanced techniques (e.g., chromatometry, chromatography, near infrared spectroscopy, laser induced breakdown spectroscopy and chemical analysis) have been used in soil nitrate-nitrogen detection and some related commercial instruments emerge[5-8], there are intrinsic limitations of practical application for precision agriculture in developing and underdeveloped countries. The characteristics of low cost, easy operation, environment-friendly, stable and durable remain the main focus in soil nutrients detection. The electrochemical sensor, which could sense specific chemical target and then convert its chemical information (concentration, activity, partial pressure) into electrical signals shows distinctive advantages in low cost, insensitivity to color and muddy, simplified operation and portability thus plays an essential role in practical applications such as environment monitoring and clinical analysis[9-10]. The conventional electrochemical sensor includes potentiometric, amperometric and impedimetric type. Ion selective electrode (ISE) a typical potentiometric electrochemical sensor presents a promising orientation in agriculture application as its merits of easy to prepare and operate, low cost, wide response range and so on[11-13]. Although the detection limit can't reach as low as 'ppb' level like amperometric and impedimetric type having, 'ppm' resolution is absolutely sufficient for general agriculture application[2]. Besides that, durability and simplicity for the follow-up detection instrument are the overwhelming superiority in developing a commercial apparatus[14]. However most of pre-existing ISEs are hollow structure with internal solution thus pose obstacles for themselves such as leakage and deterioration of the solution, mechanical fragility and position dependence in use. Therefore, a lot of research work[15-18] was launched and the all-solid-state ISEs (SS-ISEs) came out subsequently.

Conducting polymer (CP) owning an ability of selective molecular recognition to doping ions is widely used as the ion selective membrane (ISM) and ion-to-electron transducer in fabricating SS-ISEs[19-22]. However, the response potential drift is an obstinate problem especially for the SS-ISEs based on porous CP material. Thus exploring more suitable materials for ISM is imperative in SS-ISE making. Recently, some researchers speculated that a water layer formed between the ISM and substrate was a possible reason for potential drift and a new solution was proposed, which was introducing a conductive and hydrophobic solid contact layer to restrain the aqueous layer[13, 15, 23]. Graphene (GR) a two-dimensional monolayer carbon nanomaterial has gained enormous attention in

recent years as its exceptional mechanical, chemical, electronic properties. Some literatures have reported a good applicability for GR material being used as the solid contact layer to fabricate a stable SS-ISE[13, 15, 23]. Our research team also compared the performance of TG-NS (PVC film SS-ISE, GR solid contact layer, ionophore of TDDA) with PPy-NS (PPy-$NO_3^-$ film SS-ISE, no solid contact layer)[13]. Although a higher selectivity and response rate were presented for PPy-$NO_3^-$ film, the PPy-NS performance in practical application was discounted as an obvious potential drift for long time continuous use. We further found that a GR layer can't be introduced into the PPy-NS conveniently. Specifically, most of graphene used in electrochemical sensor was generated by chemical reduction method and then forming a GR layer by drop or spray-on process. However the droped film was easy to fall away from the substrate in aqueous solution especially in the electro-polymerization process. Moreover, the chemical reduction process often needs excessive toxic reducing agents (e.g., hydrazine) and dispersing agent is necessary for the drop and spray-on operation, which brings impurity contamination. Recently, a new electro-chemical reduction method was introduced to obtain GR material[24]. Besides covering the shortages that have been mentioned, the exceptional adhesiveness of the GR layer on substrate is more attractive for our work. Additionally, a suitable preparation method for combining CP with carbon nanomaterial falls short of mechanism explanation. In this regard, the sensor stability improved by composite material of PPy and GR with an appropriate method is worth studying.

In this paper, a stable nitrate SS-ISE (PPy-$NO_3^-$/GR/GCE) was prepared by electrochemically reducing a GR layer on GCE surface and electro-polymerizing a PPy film with $NO_3^-$ doping subsequently. The fabricated SS-ISE was further used to detect nitrate content in real soil samples. According to our knowledge, few papers are about the same as-prepared sensor. Results indicate that the novel electrode presents more excellent performance in soil nitrate detection than conventional SS-ISE. Furthermore, it is the first time to provide direct evidence supporting the relationship between response potential stability and hydrophobicity of solid contact layer, which offered a new method to enhance the CP performance.

## 2. MATERIALS AND METHODS

### *2.1 Reagents and instruments*

Pyrrole ($C_4H_5N$) and graphite powder (spectral pure, size<20 μm) were purchased from Sinopharm Chemical Reagent Co., Ltd (Shanghai, China). Sodium phosphate buffer (PBS) was used as supporting electrolyte to prepare GR. Sodium nitrate and nitric acid were obtained from Beijing Chemical Works (Beijing, China). High pure nitrogen was offered by Beijing Hua Yuan Gas Chemical Industry Co., Ltd (Beijing, China). Unless otherwise stated, all the reagents were analytically pure and ultrapure water (18.2 MΩ) was used for all experiments. Moreover, Pyrrole was distilled under reduced pressure before polymerization. Other reagents were used as received.

Electro-polymerization of PPy/GR composite and electrochemical measurements were carried out on an electrochemical workstation (Model CHI 660D, Shanghai, China). Surface morphology was

characterized by a field emission scanning electron microscope (JSM-6701F, JEOL Ltd., Japan). The dependable reference values of nitrate content were generated by an UV2450 ultraviolet spectrophotometer (Shimadzu, Japan). A contact angle of solid contact layer was measured by a DSA100 contact angle meter (KRUSS Co., Ltd, Germany) to characterize the wettability. Glassy carbon electrodes (GCE, Φ=3 mm) and Ag/AgCl (3 M KCl) electrode offered by Aida Co., Ltd. (Tianjin, China) were performed as substrate and reference electrode respectively. The pH value of electrolyte was monitored by a high performance pH sensor (Thermo Scientific Co., Ltd, USA) matching a M555 pH/ISE meter (Pinnacle Co., Ltd, USA ).

### *2.2 Preparation of the SS-ISEs*

GCEs were pretreated ahead by polishing with 0.5μm alumina powder then ultrasonically washing in water and alcohol alternately. Graphite oxide (GO) was then prepared according to a modified Hummers' method[25]. Subsequently, the dispersive suspension of graphene oxide was obtained by exfoliating the GO in PBS solution (0.5 M, pH 4.12) with ultrasonication. The post-pretreatment GCE was dipped into the dispersion solution and a reduction potential of -0.85 V (vs. Ag/AgCl) was applied for 15 min. After that, the GR modified electrode (GR/GCE) was acquired. It should be noted that the whole electrochemical reduction process was magnetically stirred throughout after being purged by nitrogen.

Electro-polymerization of PPy film doping with nitrate (PPy-$NO_3^-$) on the GR/GCE surface was performed in aqueous solution containing pyrrole monomer of 0.5 M and $NaNO_3$ of 1 M. The initial solution was deoxygenated by nitrogen for 10 min before polymerization and pH value was adjusted to 3 with nitric acid. After that, an impulse voltage as shown in Fig. 1 was applied to the as-prepared GR/GCE (working electrode) with a platinum plate (1×1 $cm^2$) and an Ag/AgCl electrode being used as the counter and reference electrode respectively.

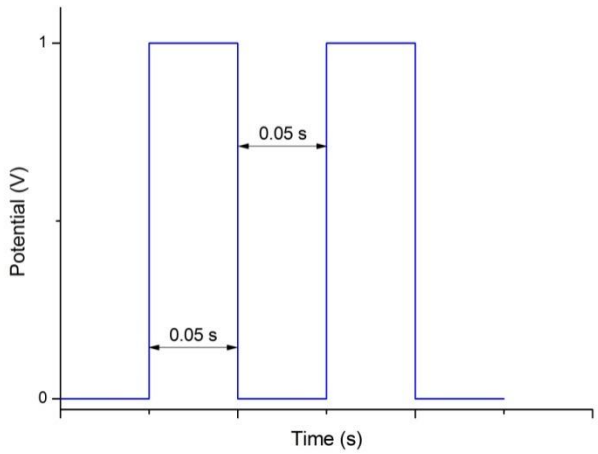


**Figure 1.** Potential waveform used in Electro-polymerization of PPy-$NO_3^-$

Total electro-polymerization time was 40 min. The whole polymerization process was in nitrogen atmosphere and bathed in water lower than 5°C. After washing with water and dried by nitrogen blowing, the PPy-$NO_3^-$/GR/GCE was finished. Before use, the SS-ISE was conditioned in $10^{-2}$ M $NaNO_3$ standard solution for at least 1 day. For comparison, the PPy-$NO_3^-$/GCEs were fabricated according to the preparation protocols above.

### *2.3 Sample preparation and measurement procedures*

65 soil samples of Beijing rural area covering high, middle and low nitrate levels were chosen. The pretreatment process was similar with a common method[13]. In brief, soil samples were dried at 60°C then crashed and sifted through a 1 mm siever. The as-prepared soil specimens were extracted to get nitrate solution, which is 10 g soil in 25 mL water then shaking 15 min and filtering with filter paper successively.

Each extraction specimen was divided into two sets. One was measured by the novel sensor and the other was used to generate a dependable reference value of nitrate content with a dual-wavelength ultraviolet spectrophotometry, which was proved to be a reliable method for nitrate detection in aqueous environment[26]. All the tests were repeated 3 times and the characterization performed in standard solutions is from low to high concentration.

## 3. RESULTS AND DISCUSSION

### *3.1 Basic characteristics of PPy-$NO_3^-$/GR/GCE*

The surface morphology difference between PPy-$NO_3^-$/GCE and PPy-$NO_3^-$/GR/GCE was illustrated by images of a scanning electron microscopy (SEM) being shown in Fig. 2. The PPy-$NO_3^-$/GCE surface presents an irregular shape of a cauliflower-like appearance, which is the typical characteristic of a common PPy film as being reported by literatures. The nodule size of oligomers is large and without an uniform magnitude. Although loosen structure and obvious gaps between granular aggregates could facilitate diffusion process, electrical conductivity would definitely be affected and an aqueous layer between PPy-$NO_3^-$ film and glassy carbon substrate may form easily. However, a compact and uniform coverage PPy-$NO_3^-$ film was generated after a GR layer was introduced. This striking change for surface morphology could be ascribed to the high conductivity of GR materials, which leads to a more homogeneous distribution for electro-polymerization charges. The uniform granule size and perfect coverage of PPy-$NO_3^-$ film indicate that a stronger interfacial interaction exists between graphene and PPy-$NO_3^-$ components, which would facilitate the formation of a stable and 3D porous materials then further increase the number of effective electro-active sites.

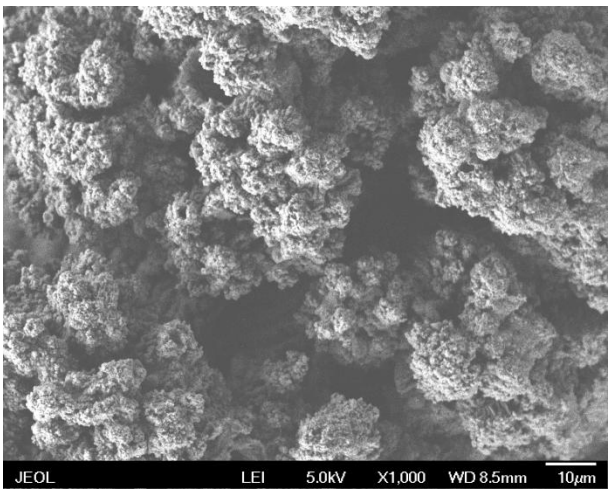


(a)

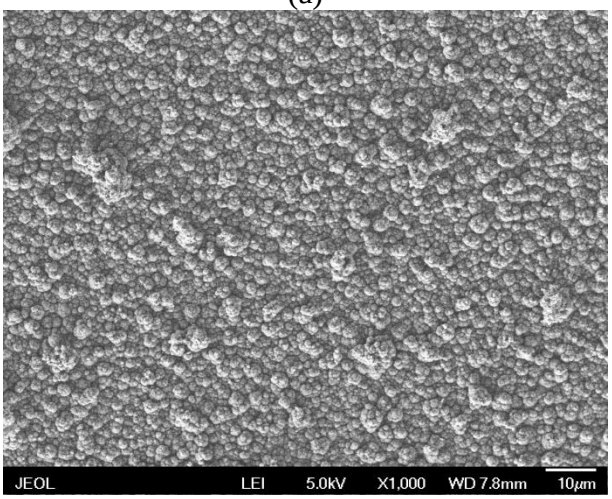


(b)

**Figure 2.** SEM images of surface morphologies (a) PPy-$NO_3^-$/GCE (b) PPy-$NO_3^-$/GR/GCE

Electrochemical impedance spectroscopy (EIS) measurement is an effective technique to characterize electron transfer kinetics and was performed in a $NaNO_3$ solution of 0.1 M (frequency, 1-1 MHz; AC modulation amplitude, 5 mV; initial voltage, open-circuit potential). Equivalent circuit was fitted by Zsimpwin software. Fig. 3 shows the nyquist plots of PPy-$NO_3^-$/GCE and PPy-$NO_3^-$/GR/GCE. In high frequency range, a distinct semicircle emerges on the respective plot, whose diameter represents the charge transfer resistance ($R_{ct}$) between interfaces. For low frequency, the appearance of a straight line denotes a linear relationship between real and imaginary parts of impedance, which is a typical characteristic for electrode process controlled by diffusion. The straight slopes of both plots are approach to 1 so a Warburg impedance (W) was employed to describe ion-diffusion resistance. For PPy-$NO_3^-$/GCE, a large semicircle was shown indicating a small capacitance in parallel with a large charge-transfer resistance at the blocked interface between GCE and ISM while a small semicircle for PPy-$NO_3^-$/GR/GCE proved an enhanced capacitance and ion-to-electron transduction at the interfaces, which illustrates that GR is a good solid contact layer and contacts well with the ISM. Fitted by the Randles equivalent circuit (inset of Fig. 3), $R_{ct}$ is 597 Ω for PPy-$NO_3^-$/GCE and 210 Ω for PPy-$NO_3^-$/GR/GCE respectively. The significant decrease indicates an improvement on

charge transfer rate after introducing GR layer, who acts as an electron-conducting tunnel. A rapid charge transfer rate would contribute to the equilibrium of phase boundary potentials for SS-ISE.

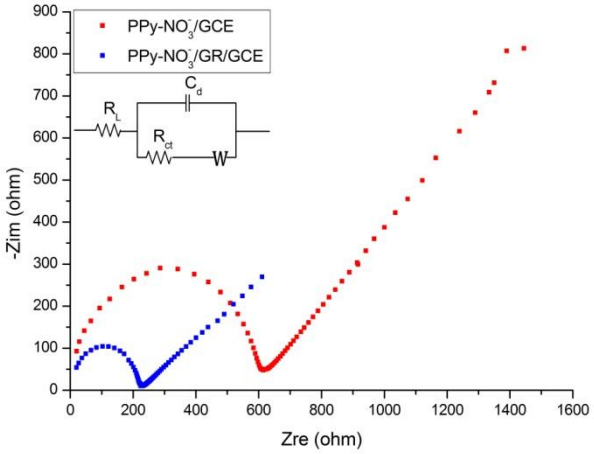


**Figure 3.** Nyquist plots of obtained sensors

The cyclic voltammograms of PPy-$NO_3^-$/GCE and PPy-$NO_3^-$/GR/GCE were compared in Fig. 4, which were measured in $NaNO_3$ solution of 0.1 M with scanning potential from -1.1 to 1 V at the scan rate of 20 $mV \cdot s^{-1}$. As shown, a couple of distinct redox peaks emerged on both curves, which were accompanied by the doping and releasing process of $NO_3^-$ as expressed by follows:

oxidation $PPy^0 \rightleftharpoons PPy^+ + e^-$ (5)

$NO_3^-$ (solution) $\rightarrow NO_3^-$ (film)

reduction $PPy^+ + e^- \rightleftharpoons PPy^0$ (6)

$NO_3^-$ (film) $\rightarrow NO_3^-$ (solution)

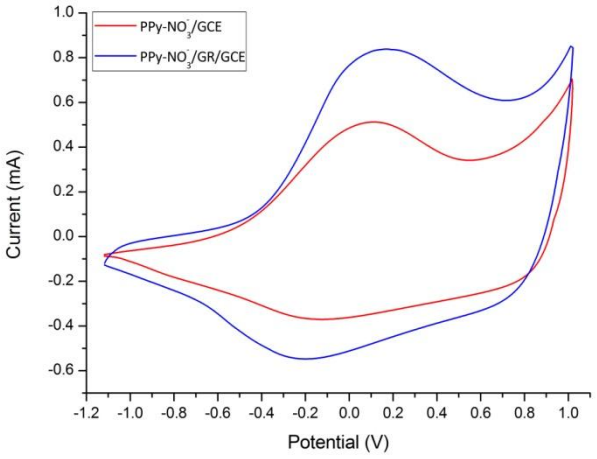


**Figure 4.** Cyclic voltammograms for PPy-$NO_3^-$/GCE and PPy-$NO_3^-$/GR/GCE

where $PPy^+$ represents oxidation state of PPy that been doped by $NO_3^-$, $PPy^0$ is eigen state of PPy which is electroneutral.

A couple of obvious redox peaks indicated that PPy-$NO_3^-$ film was electrochemically active to $NO_3^-$, which is important for a nitrate SS-ISE. For PPy-$NO_3^-$/GCE, the lower peak currents indicate a retarded electron transfer on the electrode, which could ascribe to the weak conductivity of PPy-$NO_3^-$ film. After introducing a GR layer, an enhanced redox peaks could be observed for PPy-$NO_3^-$/GR/GCE indicating an improved surface conductivity. Besides the effect of electron-conducting tunnel we have discussed above, more active sites offered by GR defects that accelerate the charge transfer behavior are the acceptable reason to peak current increase[27]. For SS-ISE, the more active sites would contribute to a lower detection limit.

### *3.2 Analytical performance of PPy-$NO_3^-$/GR/GCE*

Sensor performance (linear range, sensitivity, lowest detection limit, selectivity and response rate) was analyzed in standard nitrate solutions ranging from $10^{-7}$ to $10^{-1}$ M. Fig. 5 (a) recorded the response electromotive force vs. testing duration under an ordered increasing concentration.

A distinct step-wave voltage with a stable potential value for each step face was observed for the concentration of higher than $10^{-5}$ M. But for the nitrate of lower than $10^{-5}$ M, the sensor was insensitive to the variation of target ion content and some detectable noise appeared. Over the range of $10^{-1}$ to $10^{-5}$ M, a favorable linear relation was presented between response electromotive force and logarithmic concentration of $NO_3^-$ as showed in Fig. 5 (b), which exhibited a well Nernstian response. The calibration equation was y = (56.2±0.2) x + (32.1±1.2) with a correlation coefficient of 0.98. Sensitivity was determined by the slop of calibration curve and the detection limit. For the slope of 56.2±0.2 mV·decade$^{-1}$, it is a satisfied result that approximates to the ideal value of 59.16 mV·decade$^{-1}$ under 25°C. According to the IUPAC recommendation, the limit of detection (LOD) is determined by the intersection of two slope lines as shown in Fig. 5 (b) and was found to be $10^{-5.2\pm0.1}$ M, which is sensitive enough for soil nitrate detection in agriculture application as the general level of nitrate content in field is over 20 mg·kg$^{-1}$ (equal to $1.4\times10^{-3}$ M).

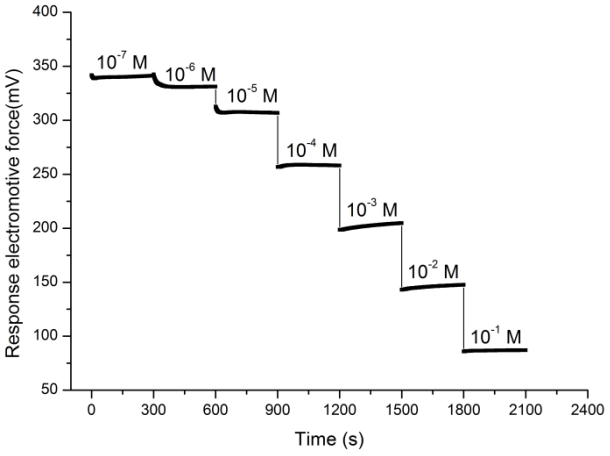


(a)

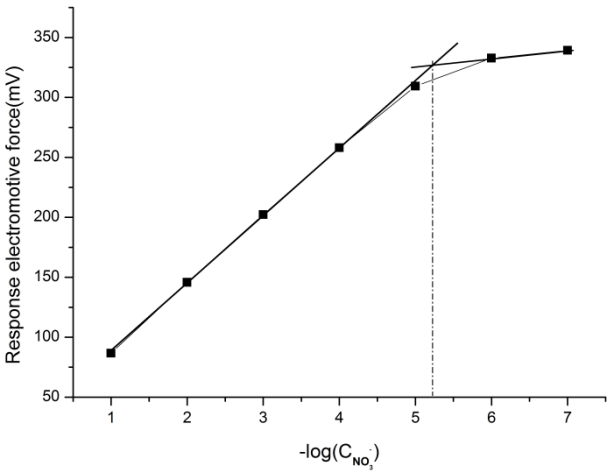


(b)

**Figure 5.** Response electromotive force of PPy-$NO_3^-$/GR/GCE (a) in standard solution and (b) calibration curve

Response rate of SS-ISE was quantified with the factor of response time, which is defined as the elapsed time between the moment of contacting with an aqueous sample and the first instant of achieving 95% of the equilibrium potential. For comparing easily, it is usually conducted in standard solution of $10^{-3}$ M and a small fluctuation of less ±1 mV is regard as timing terminal. As Fig. 6 shown, the response rate slows down with the concentration decreasing for both PPy-$NO_3^-$/GCE and PPy-$NO_3^-$/GR/GCE, which indicates that the high concentration is still a key factor for establishing a potential equilibrium. Even so, a stable potential could be reached within 15 s for PPy-$NO_3^-$/GR/GCE in the range of $10^{-5}$–$10^{-1}$ M. Compared with PPy-$NO_3^-$/GCE, response rate was enhanced significantly by introducing GR layer, which could attribute to the high conductivity and a rapid charge transfer rate as being discussed in 3.1 section.

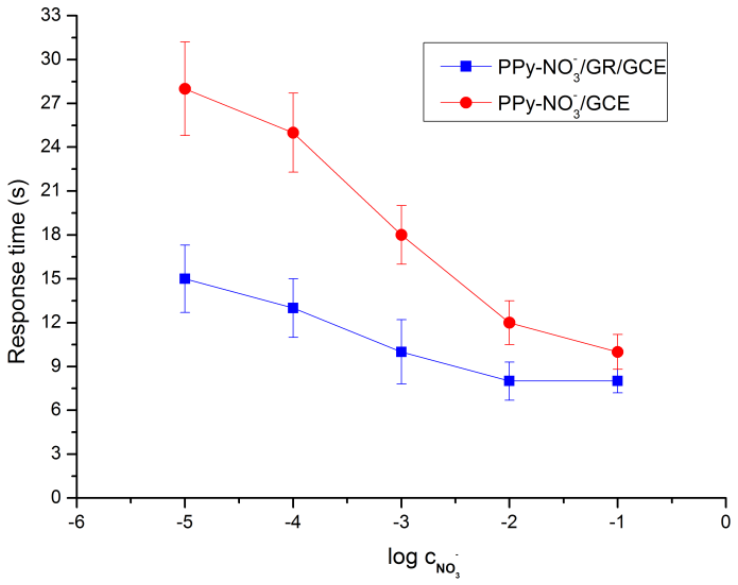


**Figure 6.** Response time test in standard solution

An ion selective electrode would also response to other ions to some extent, which are defined as the interference ions and considered as the main interference source for practical application. Selectivity coefficient ($K_{i,j}$) was used to quantify the anti-interference ability of ISE for target ion 'i' to interference ion 'j'. For convenience, the $K_{i,j}$ is usually expressed in a logarithmic form. Negative sign means more sensitive to target ion 'i' than interference ion 'j' and vice versa. Four different selectivity coefficients $\log(K_{NO_3^-,\,Cl^-})$, $\log(K_{NO_3^-,\,SO_4^-})$, $\log(K_{NO_3^-,\,H_2PO_4^-})$ and $\log(K_{NO_3^-,HCO_3^-})$ were calculated using separate solution method[28] and summarized in Tab. 1. Although there is no significant difference ($p=0.16>0.05$) for $K_{i,j}$ between PPy-$NO_3^-$/GCE and PPy-$NO_3^-$/GR/GCE, which was statistically analyzed by a paired t-test at the confidence level of 95% and $Cl^-$ is still a main interference ion, the $\log(K_{NO_3^-,\,Cl^-})$ of -2.5 and $\log(K_{NO_3^-,\,SO_4^-})$ of -4.3 are still superior to previous developed nitrate ISE as compared in Tab. 1. It also indicates that the introduction of graphene does not improve selectivity which is mainly determined by the ISM.

**Table 1.** Comparison of all-solid-state nitrate selective electrodes

| Electrode | Slop (mV·decade$^{-1}$) | Linear range (M) | Response time | Detection limit (M) | Selectivity coefficients ($\log K_{NO_3^-,j}$) | | | | References |
|---|---|---|---|---|---|---|---|---|---|
| | | | | | $Cl^-$ | $SO_4^-$ | $H_2PO_4^-$ | $HCO_3^-$ | |
| MTDDA-$NO_3$ | 57.9 | $10^{-4.3}$–$10^{-1}$ | ≤ 10 s | $3\times10^{-5}$ | -1.9 | -3.1 | / | / | [15] |
| TDMA-NO3 | 58 | $3\times10^{-5}$–$10^{-1}$ | 1 min | $10^{-5}$ | -2.2 | -3 | / | / | [29] |
| I–PVC–TBAB–DBP | 57 | $10^{-5}$–$10^{-1}$ | ≤ 20 s | $3.9\times10^{-5}$ | -1.46 | -1.3 | / | -1.5 | [30] |
| C4PE | 57.5 | $10^{-5}$–$10^{-2}$ | ≤ 10 s | $10^{-5}$ | -0.8 | -2.5 | / | / | [31] |
| PPy-$NO_3^-$/GCE | 55 | $3\times10^{-5}$–$10^{-1}$ | ≤ 20 s | $10^{-5}$ | -2.2 | -4.6 | -4.7 | -3.5 | This work |
| PPy-$NO_3^-$/GR/GCE | 56.2 | $10^{-5}$–$10^{-1}$ | ≤ 10 s | $10^{-5.2}$ | -2.5 | -4.3 | -5.1 | -3.7 | This work |

The reproducibility of PPy-$NO_3^-$/GR/GCE was evaluated in nitrate standard solution of $10^{-3}$ M by repetitive measurement. The relative standard deviation (RSD) was 3.2% and 4.6% for three times measurements of one ISE and testing once for three independent ISEs fabricated in the same batch respectively, which indicates an acceptable reproducibility of the sensor. Compared with previous developed nitrate ISE as summarized in Tab. 1, the novel sensor in this work possess a fast response rate, lower detection limit and good sensitivity.

### *3.3 Analysis for potential stability*

A potentiometric water layer test[32] was conducted to evaluate the formation of a hypothetical thin aqueous layer between PPy-$NO_3^-$ film and the ion-to-electron transducer layer. As $Cl^-$ is the main

interference ion, The water layer test consists of observing the behavior of the PPy-$NO_3^-$/GCE and PPy-$NO_3^-$/GR/GCE being dipped into solutions of 0.1 M $NaNO_3$ then in 0.1 M NaCl and then again in 0.1 M $NaNO_3$. As Fig. 7 shown, a rapid shift is found for both SS-ISEs when the primary ion is replaced by interfering ion (zone B). This suggests that the $NO_3^-$ is rapidly replaced by $Cl^-$ in the membrane. The water layer is deemed to be absent for PPy-$NO_3^-$/GR/GCE as there is no obvious drift due to the equilibrium of the interfering ion in the aqueous layer when they were shifted back to zone A again. It was also observed that for PPy-$NO_3^-$/GR/GCE the same response potential values were reached before and after contacting with the interfering ion, which proved the absence of a water layer too. Compared with the opposite results of PPy-$NO_3^-$/GCE, the high hydrophobicity of GR material might be the key factor for inhibiting a water layer formation.

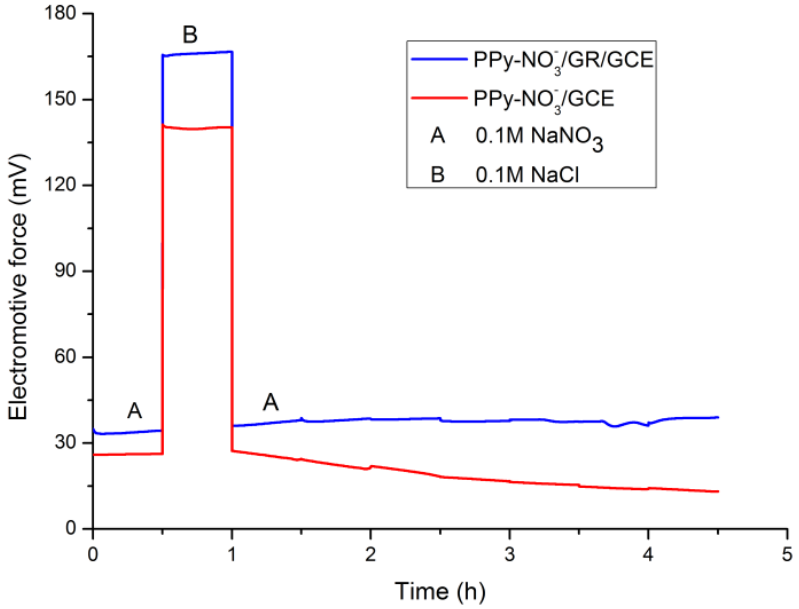


**Figure 7.** Potentiometric water layer test for PPy-$NO_3^-$/GCE and PPy-$NO_3^-$/GR/GCE

Potential stability could be further quantified by $\Delta E \cdot \Delta t^{-1}$ for continuous testing (10 hours) in $10^{-3}$ M $NaNO_3$ as the medium-term stability of electrodes[33]. For PPy-$NO_3^-$/GCE, a drift of 8.4±0.32 $mV \cdot h^{-1}$ was obtained, which was reduced to 0.67±0.05$mV \cdot h^{-1}$ for PPy-$NO_3^-$/GR/GCE. The potential stability is comparable well with the previously developed SS-ISEs based on CPs and carbon nanomaterials, whose potential drifts were almost in the range of 1.0 $mV \cdot h^{-1}$[34-37].

In order to give a direct evidence to support the speculation that the enhanced stability was related to hydrophobicity of GR layer, a contact angle (CA) measurement for GR and GCE surfaces were conducted. Each sample was tested five times at different areas to get an average value with a testing water drop of 5 μL. The results of 82±4° for GCE and 127±3° for GR surface indicate an increased hydrophobicity after introducing a GR layer as there is a positive correlationship between contact angle and hydrophobic character and hydrophobic materials were defined by the CA of more than 90°.

*3.4 Soil samples detection*

The sensor performance for practical application was evaluated by soil nitrate detection. Extract specimens of 65 soil samples being prepared as description in 2.3 were tested by PPy-$NO_3^-$/GR/GCE sensor and the time of 20 s was considered as a time criterion of equilibrium. A calibration curve of 5 standard solutions ($10^{-5}$–$10^{-1}$ M) being fitted at the beginning of the test was employed throughout. Fig. 8 shows the relationship between the sensor results and expected values measured by a dual-wavelength ultraviolet spectrophotometry.

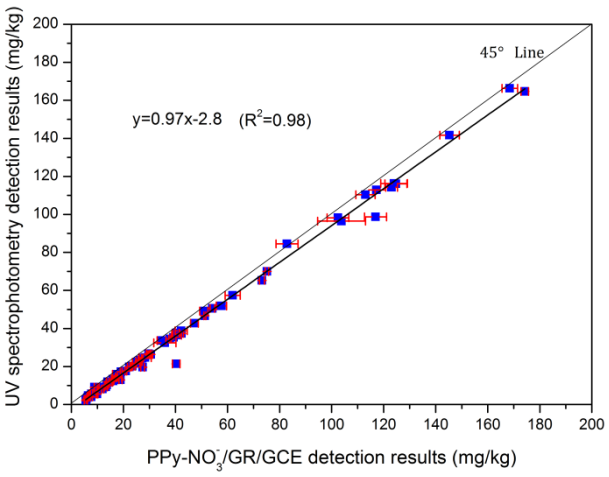


**Figure 8.** Validation of measurement results for practical soil samples

For the regression equation y=0.97x-2.8 (x: testing result, y: expected result ), a regression coefficient of 0.97 approximating to 1 and a smaller intercept value 2.8 prove a perfect consistency and an ignorable deviation of the sensor results relative to predicted values. A higher fitting degree of the regression equation was supported by the $R^2$=0.98 and the P value of 0 being analyzed by ANOVA indicated a significant linear correlation. After eliminating outliers, the relative error (RE) of soil detection ranged from 0.5–43% but only a few RE was greater than 8%. The rare RE values of larger than 20% almost completely occurred for the very low level samples (≤8 mg/kg) with higher pH value (≥ 9.3), which was ascribed probably to the interruption of the conjugation and degradation of electroactivity for PPy film as a strong overoxidation in alkaline solution. It has been accepted that the strong nucleophile of $OH^-$ is the direct reagent for the attack on the conjugated double bonds of PPy and the overoxidation is closely related to the attack of hydroxide yielding carbonyl groups[38]. Even so, for most samples the maximum relative relative error of lower than 8% was satisfying for soil detection.

Like our previous work[13], we also validated the potential stability in soil slurry samples, 3 soil samples of high, medium and low nitrate level were selected and pretreated as 2.3 section only avoiding filter process. After the sensor was immersed into soil slurry specimens, potential outputs were continuously monitored for 500 s. In the first 100 s, data was recorded at interval of 10 s to test response rate then 4 values were observed at interval of 100 s to evaluate the stability. As shown in

Fig. 9, a stable potential equilibrium could be reached within 60 s for all the soil slurry specimens and there was no obvious potential drift for the following time. An additional time of 30-45 s was needed to establish potential equilibrium in slurry environment relative to the extracted sample, which may be caused by the settlement action of tiny-particle clay. Although some perceptible error bars were presented, the calculated values of relative standard deviation were lower than 2% for the last 4 sampling potential values of each sample indicating a good practicability for fast detection applications. Compared to our previous works[13], the PPy- $NO_3^-$ /GR/GCE exhibits a great improvement on the stability for soil slurry direct measurement, which is a valuable property to in-situ detection.

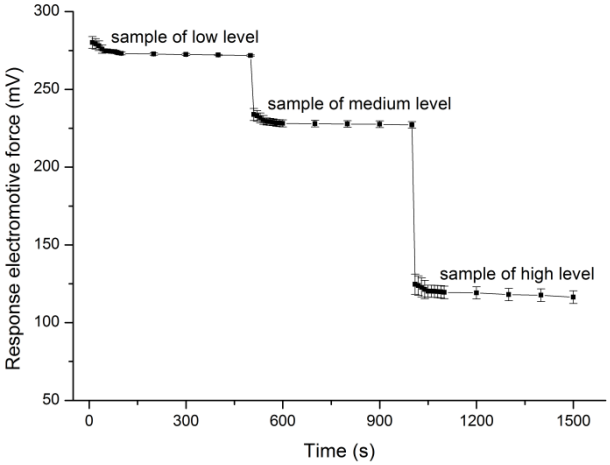


**Figure 9.** Stability of response potential for soil slurry direct measurement

All the results indicated that the sensor of PPy-$NO_3^-$/GR/GCE could be used in soil nitrate detection with a good stability.

## 4 CONCLUSION

In this paper, a stable potentiometric solid state sensor of PPy-$NO_3^-$/GR/GCE was prepared and characterized by physical and electrochemical methods. Then the sensor was employed to detect nitrate content in practical soil samples. As addition of graphene layer, the excellent properties of high conductivity and hydrophobicity were introduced to enhance sensor performance. For the novel PPy-$NO_3^-$/GR/GCE, potential response was stable, rapid and sensitive to target ion. Furthermore, an acceptable selectivity and a wide linear range meet the demand for soil macronutrients detection. The sensor will possess a fine stability for soil slurry direct measurement when a longer response time is given. Although there was no obvious improvement on LOD and anti-interference performance compared to some liquid-contact commercial sensors, our electrode was low cost, easy to fabricate, simple to use and environmentally friendly, which provided a promising method for soil nutrient detection in agriculture field.

ACKNOWLEDGMENTS
This work was financially supported by the Natural Science Foundation of China (31201136 & 61134011)

## References

1. Zhao-hui Wang, Yan-fang Miao, Sheng-xiu Li, *Field Crops Research*, 183 (2015) 211.
2. Am Jang, Zhiwei Zou, Kang Kug Lee, Chong H Ahn, Paul L Bishop, *Measurement Science and Technology*, 22 (2011) 32001.
3. Anthony Butler, *Journal of Ethnopharmacology*, 167 (2015) 105.
4. Nadia Espejo-Herrera, Kenneth P. Cantor, Nuria Malats, Debra T. Silverman, Adonina Tardón, Reina García-Closas, Consol Serra, Manolis Kogevinas, Cristina M. Villanueva, *Environmental Research*, 137 (2015) 299.
5. R.G. Gavlak, D.A. Horneck, R.O. Miller, J. Kotuby-Amacher, *Soil, plant and water reference methods for the western region*, Western Region Extension Publication, Alaska (2005).
6. Karen Y. Yamamoto, David A. Cremers, Leeann E. Foster, Mathew P. Davies, Ronny D. Harris, *Applied Spectroscopy*, 59 (2005) 1082.
7. Madhavi Z. Martin, Nicole Labbé, Nicolas André, Stan D. Wullschleger, Ronny D. Harris, Michael H. Ebinger, *Soil Science Society of America Journal*, 74 (2010) 87.
8. Yongni Shao, Yong He, *Soil Research*, 49 (2011) 166.
9. Saeid Ahmadzadeh, Majid Rezayi, Ehsan Faghih-Mirzaei, Mehdi Yoosefian, AnuarKassim, *Electrochimica Acta*, 178 (2015) 580.
10. Bárbara V. Noronha, Eduardo H. Bindewald, Michelle C. de Oliveira, Maurício A.P. Papi, Márcio F. Bergamini, Luiz H. Marcolino-Jr., *Materials Science and Engineering C*, 43 (2014) 517.
11. Li Zhou, Claude E. Boyd, *Aquaculture*, 450 (2016) 187.
12. V.I. Adamchuk, E.D. Lund, B. Sethuramasamyraja, M.T. Morgan, A. Dobermann, D.B. Marx, *Computers and Electronics in Agriculture*, 48 (2005) 272.
13. Linan Zhang, Miao Zhang, Haiyan Ren, Pan Pu, Pan Kong, Haojun Zhao, *Computers and Electronics in Agriculture*, 112 (2015) 83.
14. Johan Bobacka, Ari Ivaska, Andrzej Lewenstam, *Electroanalysis*, 34 (2013) 366.
15. Wenzhi Tang, Jianfeng Ping, Kai Fan, Yixian Wang, Xue Luo, Yibin Ying, Jian Wu, Qingli Zhou, *Electrochimica Acta*, 81 (2012) 186.
16. D.J. Walton, C.E. Hall, *Synthetic Metals*, 45 (1991) 363.
17. Artur Jasiński, Marcin Guziński, Grzegorz Lisak, Johan Bobacka, Maria Bocheńska, *Sensors and Actuators B: Chemical*, 218 (2015) 25.
18. Hilal Eren, Harun Uzun, Muberra Andac, Seda Bilir, *Journal of Food and Drug Analysis*, 22 (2014) 413.
19. Toshiyuki Goto, Takeo Hyodo, Taro Ueda, Kai Kamada, Kazunari Kaneyasu, Yasuhiro Shimizu, *Electrochimica Acta*, 166 (2015) 232.
20. Ni Hui, Shiying Wang, Hongbo Xie, Shenghao Xu, Shuyan Niu, Xiliang Luo, *Sensors and Actuators B: Chemical*, 221 (2015) 606.
21. Sakshi Sharma, Shahir Hussain, Sukhvir Singh, S.S. Islam, *Sensors and Actuators B: Chemical*, 194 (2014) 213.
22. Didem Ucan, Fulya Ekiz Kanik, Yunus Karatas, Levent Toppare, *Sensors and Actuators B: Chemical*, 201 (2014) 545.
23. Jianfeng Ping, Yixian Wang, Jian Wu, Yibin Ying, *Electrochemistry Communications*, 13 (2011) 1529.

24. Zhiqiang Wang, Hui Wang, Zhihao Zhang, Xiaojing Yang, Gang Liu, *Electrochimica Acta*, 120 (2014) 140.
25. W.S. Hummers, R.E. Offeman, *Journal of the American Chemical Society*, 80 (1958) 1339.
26. Goldman Eugene, Jacobs Richard, *Journal of American Water Works Association*, 53 (1961) 187.
27. Ming Zhou, Yueming Zhai, Shaojun Dong, *Analytical Chemistry*, 81 (2009) 5603.
28. Yoshio Umezawa, Philippe Bühlmann, Kayoko Umezawa, Koji Tohda, Shigeru Amemiya, *Pure Appl. Chem.*, 72 (2000) 1851.
29. Yu.G. Mourzina, Yu.E. Ermolenko, T. Yoshinobu, Yu. Vlasov, H. Iwasaki, M.J. Schöning, *Sensors and Actuators B: Chemical*, 91 (2003) 32.
30. Vinod Kumar Gupta, Lok Pratap Singh, Sudeshna Chandra, Sunita Kumar, Rakesh Singh, Bhavana Sethi, *Talanta*, 85 (2011) 970.
31. Naader Alizadeh, Samaneh Nabavi, *Sensors and Actuators B*, 205 (2014) 127.
32. Monia Fibbioli, Werner E. Morf, Martin Badertscher, Nicolaas F. de Rooij, Ernö Pretsch, *Electroanalysis*, 12 (2000) 1286.
33. Rafael Hernández, Jordi Riu, F. Xavier Rius, *Analyst*, 135 (2010) 1979.
34. Amr M. Mahmoud, Mohamed K. Abd El-Rahman, Mohamed R. Elghobashy, Mamdouh R. Rezk, *Journal of Electroanalytical Chemistry*, 755 (2015) 122.
35. Alemayehu P. Washe, Santiago Macho, Gastón A. Crespo, F. Xavier Rius, *Analytical Chemistry*, 82 (2010) 8106.
36. Tom Lindfors, Harri Aarnio, Ari Ivaska, *Analytical Chemistry*, 79 (2007) 8571.
37. Agata Michalska, *Analytical and Bioanalytical Chemistry*, 384 (2006) 391.
38. Tian Ying, Wang Jingri, Liu Ming, Shi Kun, Yang Fenglin, *Acta Physico-Chimica Sinica*, 27 (2011) 1116.